

SCALAR - Simultaneous Calibration of 2D Laser And Robot's Kinematic Parameters Using Three Planar Constraints

Teguh Santoso Lembono^{1,2}, Francisco Suárez-Ruiz², and Quang-Cuong Pham²

Abstract—Industrial robots are increasingly used in various applications where the robot accuracy becomes very important, hence calibrations of the robot's kinematic parameters and the measurement system's extrinsic parameters are required. However, the existing calibration approaches are either too cumbersome or require another expensive external measurement system such as laser tracker or measurement spinarm. In this paper, we propose SCALAR, a calibration method to simultaneously improve the kinematic parameters of a 6-DoF robot and the extrinsic parameters of a 2D Laser Range Finder (LRF) that is attached to the robot. Three flat planes are placed around the robot, and for each plane the robot moves to several poses such that the LRF's ray intersect the respective plane. Geometric planar constraints are then used to optimize the calibration parameters using Levenberg-Marquardt nonlinear optimization algorithm. We demonstrate through simulations that SCALAR can reduce the average position and orientation errors of the robot system from 14.6 mm and 4.05° to 0.09 mm and 0.02°.

I. INTRODUCTION

In traditional robotics applications such as pick and place, spray-painting and spot-welding, the robots either do not need very high accuracy or they are programmed by teaching, where the **repeatability** of the robot is more important than the **accuracy**. Repeatability refers to the robot's capability to return precisely to the same location as previously taught, whereas accuracy refers to the robot's capability to precisely reach a pose computed based on the robot's kinematic model.

However, there are many applications where the accuracy of the robot becomes very crucial, given that the robot has to adapt to each task automatically with a great precision. Consider, for example, a robot drilling task in [1] where the robot is required to drill several holes at precisely-defined locations on a workpiece. The workpiece can be different for each task, and the placement within the workspace may not be precisely known. To program the robot automatically for such task, the robot has to do a few things accurately: the robot has to scan the workpiece, determine the location of the holes, and finally move to that location accurately. The accuracy of such a robotic system depends on at least two things: The accuracy of the robot and the accuracy of the measurement system.

The accuracy of the robot is determined by how closely the kinematic parameters of the robot's model resemble the actual kinematic parameters of the physical robot. This is affected by the manufacturing process, the assembly process, and the wear and tear during the operation of the robot.

¹ Idiap Research Institute, Martigny, Switzerland ² School of Mechanical and Aerospace Engineering, Nanyang Technological University, Singapore.

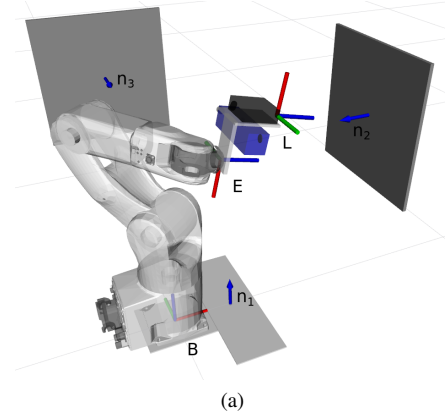


Fig. 1. Calibration Setup

Robot kinematic calibration is usually conducted to achieve a better accuracy, either by using an external measurement system (such as motion capture system or coordinate measuring machines) or by constraining the motion of the end-effector.

The accuracy of the measurement system can be divided into two parts: the accuracy of the measurement device itself and the accuracy of its **extrinsic parameters** (i.e. the relative pose between the robot and the measurement system coordinate frame). The accuracy of the measurement device depends on the type of device that is used and its specification. For example, a camera system is generally less precise as compared to a laser system, although a camera can give more information. The accuracy of the extrinsic parameters can be improved by doing **extrinsic calibration** of the measurement system.

In this paper we present SCALAR, a calibration method to simultaneously improve the accuracy of the robot and the measurement system. SCALAR calibrates simultaneously the kinematic parameters of the robot and the extrinsic parameters of a 2D Laser Range Finder (LRF) using only the information provided by the LRF attached to the robot's flange. An LRF is chosen because it gives very accurate measurement data both for the calibration and for the subsequent tasks (such as drilling).

The overall calibration procedure is as follows:

- 1) The LRF is attached to the robot and three perpendicular flat planes are placed around the robot (Fig. 1).
- 2) For each plane, the robot is moved to several poses such that the LRF's 2D ray is projected onto the plane. The LRF data and the robot's joint angles are collected.
- 3) An optimization algorithm is used to find the optimal

TABLE I
EXAMPLES OF UNCONSTRAINED CALIBRATION

Researchers	Robot	Measurement Device	Initial Accuracy[mm]	Final Accuracy[mm]
Ginani and Mota [2]	ABB IRB 2000	ROMER Measurement Arm	2.20	1.40
Ye et al. [3]	ABB IRB 2400/L	Faro Laser Tracker	1.764	0.640
Nubiola and Bonev [4]	ABB IRB 1600-6/1.45	Faro Laser Tracker ION	2.158	0.696
Newman et al. [5]	Motoman P-8	SMX Laser Tracker	3.595	2.524

robot’s kinematic parameters and the LRF’s extrinsic parameters, using the geometric constraint that the projected LRF data should be located on the three planes.

The remainder of the paper is as follows. In Section II we discuss the existing approaches to the calibration problem for robot’s kinematic parameters and LRF’s extrinsic parameters, and how SCALAR differs from the other approaches. In Section III, SCALAR is explained in detail. A simulation study is presented in Section IV to verify SCALAR, and finally we conclude with a few remarks in Section V.

II. RELATED WORKS

A. Calibration of robot’s kinematic parameters

Robot kinematic calibration has been researched for a long time; some of the earliest works began in 1980s. The calibration procedures can be categorized into **unconstrained** and **constrained** calibration. In **unconstrained calibration**, the robot moves its end-effector to several poses while an external measurement system measures the pose. The measured pose is then compared to the one computed from the kinematic model, and the model is updated to minimize the difference between the predicted pose and the measured pose. In **constrained calibration**, some constraints are applied to the motion of the end-effector, and the constraints yield several calibration equations by which the robot’s kinematic parameters are calibrated.

Examples of unconstrained calibration works can be seen in Table I. The issues with such calibration method are the difficulty in setting up the calibration setup and the expensive cost of the external measurement system. For example, the cost of a laser tracker is more than \$100,000 USD [4]. Therefore, many researchers try to find calibration methods which only rely on the internal sensors of the robot by constraining the motion of the end-effector such as in constrained calibration.

In [6], Ikits and Hollerbach propose a kinematic calibration method using a planar constraint. A touch probe attached to the robot’s flange is moved to touch random points on a plane. When the touch probe is in contact with the plane, the joint angles are recorded. The kinematic parameters of the robot model are then updated to satisfy the planar constraint. While the approach is promising, they also report that some of the parameters are hardly observable (i.e. cannot be obtained accurately) when the measurements are noisy or when the model is not complete.

In [7], Zhuang et al. investigate robot calibration with planar constraints, in particular the observability conditions

of the robot’s kinematic parameters. They prove that a single-plane constraint is insufficient for calibrating a robot, and a minimum of three planar constraints are necessary. Using three planar constraints, the constrained system is proved to be equivalent to an unconstrained point-measurement system under three conditions: a) All three planes are mutually non-parallel, b) the identification Jacobian of the unconstrained system is nonsingular, and c) the measured points from each individual plane do not lie on a line on that plane. They verify the theory by doing a simulation on a PUMA560 robot.

In [8], Joubair and Bonev calibrated both the kinematic and non-kinematic (stiffness) parameters of a FANUC LR Mate 200iC industrial robot by using four planar constraints, in the form of a high precision 9-inches granite cube. The cube’s surfaces are flat to within 0.002 mm). The robot is equipped with an MP250 Renishaw touch probe which is moved to touch four sides of the granite cube. They improved the maximum plane error from 3.740 mm to 0.083 mm.

B. Calibration of extrinsic 2D LRF parameters

Extrinsic calibration of an LRF consists of finding the precise homogeneous transformation from the robot coordinate frame to the laser coordinate frame. Most of the works on extrinsic calibration of an LRF involves a camera, since both sensors are often used together in many applications. The works in this field are largely based on Zhang and Pless’ work [9]. They propose a method to calibrate both a camera and an LRF using a planar checkerboard pattern. First, the camera is calibrated by a standard hand-eye calibration [10] using the checkerboard pattern. The calibrated camera is then used to calculate the pose of the pattern. Next, the robot is moved to several poses with the LRF pointing to the pattern. By using the geometric constraints that all the data points from the LRF should fall on the pattern plane, the extrinsic parameters of the LRF can be obtained. Finally, the same constraints are used to optimize both the intrinsic and extrinsic parameters of the camera and the extrinsic parameters of the LRF. The nonlinear optimization problem is solved by using Levenberg-Marquardt optimization algorithm.

Unnikrishnan and Hebert [11] use the same setup as [9], although they do not optimize the camera parameter simultaneously due to the nonlinearity of the resulting cost function. Li et al. [12] use a specially designed checkerboard to calibrate the extrinsic parameters between a camera and an LRF, and claim that the result is better than [9]. Vasconcelos et al. [13] develop a minimal closed-form solution for the extrinsic calibration of a camera and an LRF, based on the work in [9].

C. Novelty of the proposed method

SCALAR can be seen as a combination of the algorithm for extrinsic calibration of an LRF [9] and the algorithm for calibration of robot's kinematic parameters using three planar constraints [8]. It has the following advantages as compared to the other calibration approaches:

- 1) SCALAR simultaneously calibrates both the LRF's extrinsic parameters and the robot's kinematic parameters. Since calibration is often cumbersome, this saves a lot of time and effort. Moreover, the errors in the robot's kinematic parameters affect the extrinsic calibration accuracy and vice versa, so calibrating both parameters simultaneously results in better accuracy.
- 2) SCALAR does not need an additional camera to calibrate the LRF, unlike [9].
- 3) SCALAR does not need another expensive external measurement system. The measurement is done using the LRF that will be used in the subsequent robot task, hence it does not incur additional cost. Moreover, an LRF can give very high accuracy at much lower cost (more than ten times cheaper) as compared to the commonly used measurement systems such as Vicon or Faro Laser Tracker.
- 4) SCALAR does not need a precisely manufactured calibration object such as the granite cube in [8]. SCALAR only requires three flat surfaces which are oriented roughly perpendicular to each other and the rough estimate of their locations.
- 5) The calibration poses can be distributed throughout the whole workspace, instead of being confined only in a local region such as in [8].

III. METHOD

The calibration setup is depicted in Fig. 1, where three roughly perpendicular planes ($k = 1, 2, 3$) are placed around the robot. An LRF is attached to the robot flange. For each plane, the robot is moved to N poses such that the LRF's ray is directed to the respective plane. One data set from the LRF consists of hundreds of data points, so M data points are randomly selected from the LRF data for each pose, and the robot's joint angles are recorded.

This section describes the calibration algorithm. First, the initial estimate of the LRF's extrinsic parameters is obtained using the linear least-squares method with the data from one of the planes. This is based on the algorithm in [9], although presented differently for better clarity. After that, the robot's kinematic parameters and the LRF's extrinsic parameters are optimized simultaneously to satisfy the three planar constraints using Levenberg-Marquardt nonlinear optimization method. Finally, we explain how Singular Value Decomposition (SVD) can be used to analyse which calibration parameters are identifiable, and the steps to handle the unidentifiable parameters are then presented.

A. Initial Estimate of the LRF Extrinsic Parameters

To obtain an initial estimate of the LRF's extrinsic parameters, only the data from one plane is necessary. Arbitrarily,

the bottom plane P_1 is chosen. The extrinsic parameters of the LRF ${}^E T_L$, i.e. the homogeneous transformation from the robot flange coordinate frame to the LRF coordinate frame, is estimated by the following calculations.

Let the subscript/superscript B , E , and L denote the coordinate frame of the robot base, the robot flange, and the LRF, while the subscript i , j , and k refer to the LRF data point index, the robot pose index, and the plane index respectively. Let \mathbf{p}_{ji} be one of the data points from the LRF which lies on the P_1 , \mathbf{n}_1 be the normal unit vector of P_1 , and l_1 be the perpendicular distance from the origin of the robot coordinate system to P_1 . Since \mathbf{p}_{ji} is located on the P_1 , it has to satisfy the following constraint,

$${}^B \mathbf{n}_1^T {}^B \mathbf{p}_{ji} - {}^B l_1 = 0. \quad (1)$$

${}^B \mathbf{p}_{ji}$ depends on the robot pose ${}^B T_{E,j}$ at pose index j and the LRF's extrinsic parameter ${}^E T_L$, so (1) can be expanded,

$${}^B \mathbf{n}_1^T {}^B T_{E,j} {}^E T_L {}^L \mathbf{p}_{ji} - {}^B l_1 = 0. \quad (2)$$

${}^B \mathbf{n}_1$ and ${}^B l_1$ are known approximately ($[0 \ 0 \ 1 \ 0]$ and 0.0), ${}^B T_{E,j}$ can be computed from the robot's joint angles at pose index j , and ${}^L \mathbf{p}_{ji}$ is obtained from the laser. Let

$$\mathbf{n}'_j = {}^B \mathbf{n}_1^T {}^B T_{E,j} = \begin{bmatrix} n'_{j,1} & n'_{j,2} & n'_{j,3} & n'_{j,4} \end{bmatrix}, \quad (3)$$

$$\text{then } \mathbf{n}'_j{}^T {}^E T_L {}^L \mathbf{p}_{ji} - {}^B l_1 = 0. \quad (4)$$

The only unknown in (4) is ${}^E T_L$ which has 12 elements r_{uv} , where u and v denote the column and the row index of the matrix. Note that the fourth row of ${}^E T_L$ only consists of 0 and 1. Without loss of generality, let's assume that the data points from the LRF lie on the XZ planes of the laser frame L , so ${}^L \mathbf{p}_{ji} = [{}^L p_{i,x} \ 0 \ {}^L p_{i,z} \ 1]$. If we expand (4) and rearrange such that the components of ${}^E T_L$ are stacked together as a vector Φ_L , we have

$$\mathbf{x}_{ji}{}^T \Phi_L = {}^B l_1 - n'_{j,4}, \quad (5)$$

$$\text{where } \mathbf{x}_{ji} = \begin{bmatrix} {}^L p_{i,x} n'_{j,1} & {}^L p_{i,x} n'_{j,2} & {}^L p_{i,x} n'_{j,3} & {}^L p_{i,z} n'_{j,1} & {}^L p_{i,z} n'_{j,2} & {}^L p_{i,z} n'_{j,3} & n'_{j,1} & n'_{j,2} & n'_{j,3} \end{bmatrix}^T$$

$$\text{and } \Phi_L = [r_{11} \ r_{21} \ r_{31} \ r_{13} \ r_{23} \ r_{33} \ r_{14} \ r_{24} \ r_{34}]^T.$$

For each data point i , we obtain such equation as in (5). With M data points per pose and a total of N robot poses, there are NM such equations. The equations can be stacked together to form the following matrix equation,

$$\mathbf{X} \Phi_L = \mathbf{D}, \quad (6)$$

$$\text{where } \mathbf{X} = [\mathbf{x}_{11} \ \cdots \ \mathbf{x}_{1M} \ \mathbf{x}_{21} \ \cdots \ \mathbf{x}_{2M} \ \cdots \ \mathbf{x}_{NM}]^T$$

$$\text{and } \mathbf{D} = \begin{bmatrix} {}^B l_1 - n'_{1,4} & \cdots & {}^B l_1 - n'_{1,4} & {}^B l_1 - n'_{2,4} \\ \cdots & {}^B l_1 - n'_{2,4} & \cdots & {}^B l_1 - n'_{N,4} \end{bmatrix}^T.$$

Equation (6) can be solved by a linear least-square procedure to obtain Φ_L . ${}^E\mathbf{T}_L$ can then be computed from Φ_L as follows:

- 1) The parameters $[r_{11} \ r_{21} \ r_{31}]^T$ and $[r_{13} \ r_{23} \ r_{33}]^T$ are required to be unit vectors, so they have to be normalized. They constitute the first and the third column of the matrix ${}^E\mathbf{T}_L$.
- 2) The parameters $[r_{14} \ r_{24} \ r_{34}]^T$ constitute the position component of the matrix ${}^E\mathbf{T}_L$ (the 4th column).
- 3) The parameters $[r_{12} \ r_{22} \ r_{32}]^T$ can be calculated as the cross product of $[r_{13} \ r_{23} \ r_{33}]^T$ and $[r_{11} \ r_{21} \ r_{31}]^T$.

${}^E\mathbf{T}_L$ has 12 parameters, but only 6 parameters are independent. To reduce the redundancy in the subsequent steps, the rotation part of ${}^E\mathbf{T}_L$ is represented by the axis-angle representation $[r_x \ r_y \ r_z \ r_\theta]$, while the position part is represented by $[p_x \ p_y \ p_z]$.

B. Optimizing both the LRF Extrinsic Parameters and Robot's Kinematic Parameters

In the second step, the data from all the three planes are used to optimize the extrinsic parameters of the LRF, the robot's kinematic parameters and the plane parameters. The objective function is described as follows:

$$f(\Phi) = \sum_{k=1}^3 \sum_{j=1}^N \sum_{i=1}^M ({}^B\mathbf{n}_k^T {}^B\mathbf{p}_{ji} - {}^B l_k)^2 \quad (7)$$

The parameters Φ consist of the following:

- 1) Robot's kinematic parameters. We use **DH** parameters [14] $[a_i, \alpha_i, \theta_i, d_i], i = 1, 2, \dots, 6$ to represent the robot's kinematics, so there are 24 **DH** parameters for a 6-DoF robot arm.
- 2) LRF's extrinsic parameters. As mentioned in the previous section, we use the axis angle representation for the rotation part $[r_x \ r_y \ r_z \ r_\theta]$, and $[p_x \ p_y \ p_z]$ for the position part.
- 3) Plane parameters. Each plane can be described by a unit vector $[{}^B n_{k,x} \ {}^B n_{k,y} \ {}^B n_{k,z}]$ normal to the plane and its perpendicular distance from the robot base's coordinate system origin ${}^B l_k$, so there are 12 parameters for 3 planes.

In total, there are 43 parameters to be optimized. The optimization problem is then solved using a Levenberg-Marquardt nonlinear optimizer [15]. The objective function $f(\Phi)$ uses the geometric constraints that all data points from the LRF have to fall on the respective plane. Zhuang et al. [7] prove that a calibration process with such constraints is equivalent to the calibration of a robot using end-point measurement in unconstrained calibration.

For the unit vector parameters $([r_x \ r_y \ r_z]$ and $[{}^B n_{k,x} \ {}^B n_{k,y} \ {}^B n_{k,z}])$, the following constraints are added to the optimization solver:

$$r_z = \sqrt{1 - r_x^2 - r_y^2} \quad (8)$$

$${}^B n_{k,z} = \sqrt{1 - {}^B n_{k,x}^2 - {}^B n_{k,y}^2} \quad (9)$$

TABLE II
DH PARAMETERS OF DENSO VS060

i	α_i [°]	a_i [mm]	θ_i [°]	d_i [mm]
1	0.0	0.0	θ_1	345.0
2	-90.0	0.0	$\theta_2 - 90.0$	0.0
3	0.0	305.0	$\theta_3 + 90.0$	0.0
4	90.0	-10.0	θ_4	300.0
5	-90.0	0.0	θ_5	0.0
6	90.0	0.0	θ_6	70.0

C. Identifiability of the calibration parameters

Depending on the chosen robot calibration poses and the robot's kinematic model, some of the calibration parameters might not be observable due to the linear dependency among the parameters. This is a critical problem in calibration, as it will result in some of the parameters assuming erratic values which gives us unstable calibration result. To prevent that, we have to first analyse which calibration parameters are identifiable and which are not.

Following the approach in [8] and [16], SVD is applied on the identification Jacobian matrix \mathbf{J} . \mathbf{J} can be computed as follows. Let $f_{kji}(\Phi)$ be the geometric constraint equation on the data point i at the robot pose j and on the plane k ,

$$f_{kji}(\Phi) = {}^B \mathbf{n}_k^T {}^B \mathbf{p}_{ji} - {}^B l_k = 0. \quad (10)$$

Then \mathbf{J} can be computed by differentiating (10) for all the data points $i = 1, \dots, M$ at the robot poses $j = 1, \dots, N$ and for all the planes $k = 1, 2, 3$, then stack them together as a matrix,

$$\mathbf{J} = \left[\frac{\partial f_{111}(\Phi)}{\partial \Phi} \quad \frac{\partial f_{112}(\Phi)}{\partial \Phi} \quad \dots \quad \frac{\partial f_{3MN}(\Phi)}{\partial \Phi} \right]^T. \quad (11)$$

We can then apply SVD to the matrix $\mathbf{J} = \mathbf{U}\Sigma\mathbf{V}^T$. Note that for this identification step, the parameters $[r_z \ {}^B n_{1,z} \ {}^B n_{2,z} \ {}^B n_{3,z}]$ are excluded from the parameters vector Φ , since those four parameters are obtained as linear combinations of other parameters (Equation (8) and (9)). That leaves us with $43 - 4 = 39$ parameters in Φ , which correlate to the 39 singular values in Σ . The number of zero singular values in Σ is then equal to the number of unidentifiable parameters in the calibration procedure. For a given zero-value singular value σ_r , the r th column vector of the matrix \mathbf{V} is the linear combination of the parameters Φ which cannot be identified independently.

In this paper, we use a Denso VS060 6-DoF industrial manipulator with its **DH** parameters presented in Table II. The LRF's frame is defined such that the rotation part $[r_x \ r_y \ r_z \ r_\theta] = [0 \ 0 \ 1 \ \pi]$, and the position part $[p_x \ p_y \ p_z] = [-0.1275 \ -0.033 \ 0.1015]$. Applying the identifiability analysis to the system, we found that there are 7 sets of linearly dependent parameters.

- 1) The parameters d_6 (the translation along the z-axis of the 6th link frame on the flange) and p_z (the z coordinate of the LRF's frame) are linearly dependent. Physically this means that if we shift the origin of the 6th link's frame in its z direction by changing d_6 , we can

compensate by shifting the origin of the LRF's frame in the opposite direction by changing p_z .

- 2) The parameters θ_6 and r_θ are linearly dependent. These correspond to the rotation of the 6th link's frame and the rotation of the LRF's frame around the same z-axis.
- 3) The parameters d_2 and d_3 are linearly dependent. These correspond to the shift in the z-axis direction of the 2nd and 3rd link's frames respectively, which are along the same direction.
- 4) Lastly, we have four sets of linearly dependent parameters due to the linear combinations of the first link's DH parameters $[a_1, \alpha_1, \theta_1, d_1]$ and the three calibration planes' parameters. Physically, this relates to the fact that we can shift the robot's base frame freely by changing the value of $[a_1, \alpha_1, \theta_1, d_1]$, and the plane parameters will adjust according to the new base location. In other words, the base coordinate is not constrained (floating base).

For each set of the linearly dependent parameters, we can assign a fix value to one of the parameters. In this case, we fix the value of the parameters $[d_6, \theta_6, d_2, a_1, \alpha_1, \theta_1, d_1]$ to their initial model's values.

These results apply to most existing 6-DoF industrial robots whose kinematic configurations are the same as that of our Denso robot.

IV. SIMULATION

We verify SCALAR through simulation of the calibration procedure. The simulation is conducted by using Robot Operating System and Gazebo where the robot model, the LRF, and the three planes can be simulated. As shown in Fig. 1, three perpendicular planes are located around the robot, and the robot is moved such that the LRF's ray intersects each plane. Simulated data from the LRF can be obtained and Gaussian noise with zero mean and standard deviation σ_{noise} can be added to the data. The data is then used as input to the calibration algorithm. The optimization is typically completed in less than 15 s using Python.

After the calibration, the robot is moved to 10,000 random poses to evaluate the accuracy of the calibrated parameters. Let ${}^B\mathbf{T}_{L,j,\text{true}}$ and ${}^B\mathbf{T}_{L,j,\text{model}}$ be the true and calibrated pose of the LRF's frame w.r.t. the robot base frame at the robot pose index j , respectively, then the error of the calibrated model can be computed as

$$\Delta\mathbf{T}_j = {}^B\mathbf{T}_{L,j,\text{model}}^{-1} {}^B\mathbf{T}_{L,j,\text{true}}. \quad (12)$$

Let δt_{uv} be the element of $\Delta\mathbf{T}_j$ with the subscript u and v refer to the row and column index, then **the position error** at the robot pose index j , δp_j , can be computed by

$$\delta p_j = \sqrt{\delta t_{14}^2 + \delta t_{24}^2 + \delta t_{34}^2}. \quad (13)$$

Let $\delta\mathbf{R}_j$ be the rotation part of the homogeneous transformation matrix $\Delta\mathbf{T}_j$. $\delta\mathbf{R}_j$ can be represented by using an axis-angle notation, $[r_{j,1} \ r_{j,2} \ r_{j,3} \ \delta\theta_j]$. We use $\delta\theta_j$ as **the orientation error** at the robot pose index j . $\delta\theta_j$ can be seen as the amount of rotation necessary to rotate the

calibrated pose to the true pose. The errors δp_j and $\delta\theta_j$ are then averaged over the 10,000 random poses.

The simulated robot's model is considered as having the true kinematics and extrinsic parameters, and an initial model is generated by introducing random Gaussian errors to the true parameters within the range of ± 2 mm and $\pm 1^\circ$ for the linear and angular parameters, respectively. Note that the initial model's errors are intentionally set to be large to illustrate the robustness of the calibration method. The average position and orientation errors of the initial model as compared to the true model are 14.6 mm and 4.05° , while the maximum errors are 103.9 mm and 5.95° . We run the calibration procedure to improve the initial model with $3N = 120$, $M = 100$ and $\sigma_{\text{noise}} = 0.1$ mm, and the resulting calibrated model has the average position and orientation errors reduced to 0.09 mm and 0.02° , while the maximum errors are reduced to 0.19 mm and 0.035° .

Next, we evaluate the effect of the measurement noise, the number of poses (N) and points (M), and the plane parameters' initial estimate on the calibration errors.

A. Effect of the measurement noise

The accuracy of the calibration procedure depends greatly on the accuracy of the measurement system, which is affected by the noise on the data. In this section, Gaussian noise with zero means and varying standard deviations σ_{noise} are added to the measurement data in the simulation, and its effect on the calibration errors is shown in Fig. 2a. As σ_{noise} decreases, the calibration errors decrease. At $\sigma_{\text{noise}} = 0.1$ mm, the average position and orientation errors are around 0.1 mm and 0.02° , respectively. For the subsequent sections, σ_{noise} is set at 0.1 mm.

B. Effect of the number of calibration poses and the number of points

For each plane, the robot is moved to N poses, so in total there are $3N$ calibration poses. At each pose, we select M data points from the LRF data. In this section we evaluate the effect of $3N$ and M to the calibration errors. In Fig. 2b, it can be seen that as the number of poses $3N$ increases, the error decreases until around $3N = 60$, beyond which it does not change significantly. It can be concluded that 60 robot poses are sufficient to calibrate the robot model accurately. We also conduct similar analysis on M (not presented in this paper) and found that $M = 20$ is sufficient for the calibration.

C. Effect of the plane parameters' initial estimate

One of the advantages of SCALAR is that the plane parameters do not need to be precisely known. Here the plane parameters' estimate is varied to demonstrate the method's robustness. The initial estimates of the positions and the normals of the planes are disturbed by up to 100 mm and 30° , as shown in Fig. 2c and Fig. 2d. From the figures, it can be seen that the calibration position and orientation errors are not affected by the errors in the plane parameters' initial estimate. In fact, after calibration, the plane parameters in the calibrated model approach the true parameters within 0.1 mm and 0.01° .

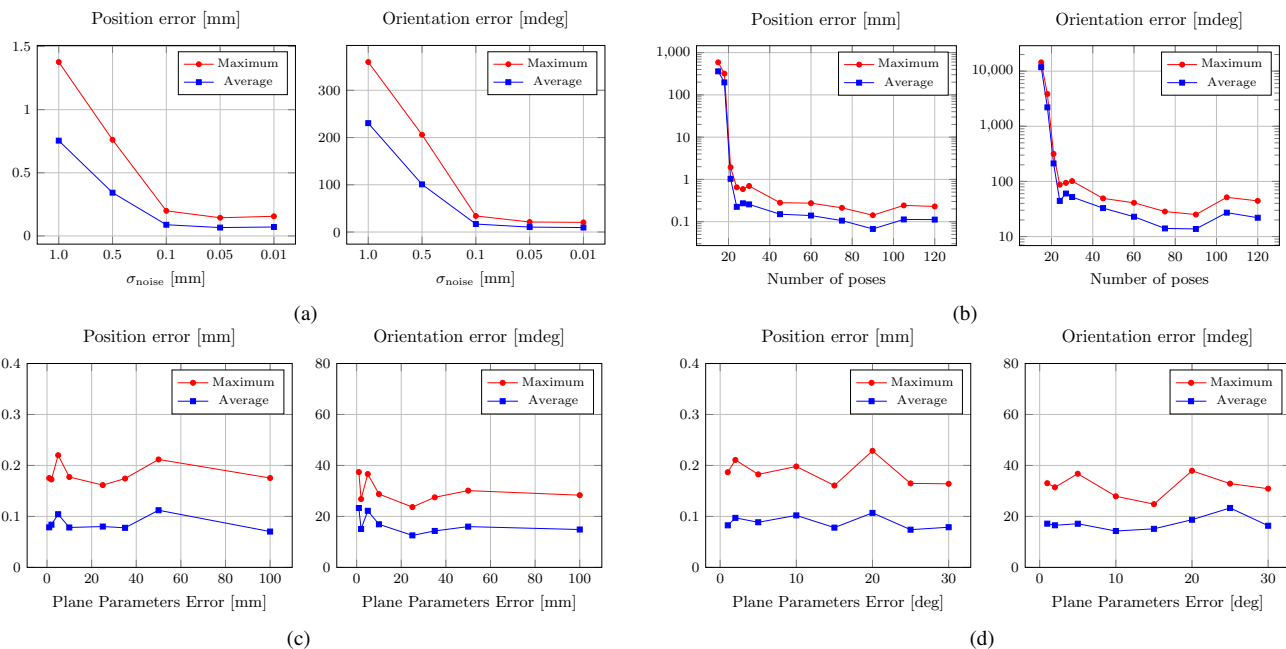


Fig. 2. Effect of a) the measurement noise, b) the number of poses, c) planes' position estimate error, and d) plane's orientation estimate error towards the position and orientation error after calibration

V. CONCLUSIONS

In this paper, we have proposed SCALAR, a method to simultaneously calibrate a 6-DoF robot's kinematic parameters and a 2D LRF's extrinsic parameters using only three flat planes, arranged perpendicularly towards each other around the robot. SCALAR is easier to implement than the previous methods in the literature as it does not require other expensive measurement systems or tedious setup. We have verified from simulations that the method reduces the average errors in position and orientation from (14.6 mm, 4.05°) to (0.09 mm, 0.02°), respectively. This is very useful for many industrial robotics applications that require great accuracy.

The next step is to implement SCALAR on the real system. Some challenges that may appear on the real system are the backlash of the robot's transmission system, the elasticity of the joints, the roughness of the calibration planes and the noise of the LRF data which will reduce the calibration accuracy. We will present the calibration result on the real system in our future work.

ACKNOWLEDGMENT

This work was supported in part by NTUitive Gap Fund NGF-2016-01-028, SMART Innovation Grant NG000074-ENG, and the European Union under the EU H2020 collaborative project MEMMO (Memory of Motion), Grant Agreement No. 780684.

REFERENCES

- [1] F. Suárez-Ruiz, T. Santoso Lombono, and Q.-C. Pham, "RoboTSP: A Fast Solution to the Robotic Task Sequencing Problem," in *International Conference on Robotics and Automation*, 2018.
- [2] L. S. Ginani and J. M. S. T. Motta, "Theoretical and practical aspects of robot calibration with experimental verification," *Journal of the Brazilian Society of Mechanical Sciences and Engineering*, vol. 33, no. 1, pp. 15–21, 2011.
- [3] S. H. Ye, Y. Wang, Y. J. Ren, and D. K. Li, "Robot calibration using iteration and differential kinematics," *Journal of Physics: Conference Series*, vol. 48, no. 1, pp. 1–6, 2006.
- [4] A. Nubiola and I. A. Bonev, "Absolute calibration of an ABB IRB 1600 robot using a laser tracker," *Robotics and Computer-Integrated Manufacturing*, vol. 29, no. 1, pp. 236–245, 2013.
- [5] W. S. Newman, C. E. Birkhimer, R. J. Horning, and A. T. Wilkey, "Calibration of a Motoman P8 robot based on laser tracking," in *Proceedings-IEEE International Conference on Robotics and Automation*, vol. 4, 2000, pp. 3597–3602.
- [6] M. Ikits and J. Hollerbach, "Kinematic calibration using a plane constraint," *Proceedings of the 1997 International Conference on Robotics and Automation*, vol. 2, no. 4, pp. 3191–3196, 1997.
- [7] H. Zhuang, S. Motaghedi, and Z. Roth, "Robot calibration with planar constraints," *Proceedings 1999 IEEE International Conference on Robotics and Automation*, vol. 1, pp. 805–810, 1999.
- [8] A. Joubair and I. A. Bonev, "Non-kinematic calibration of a six-axis serial robot using planar constraints," *Precision Engineering*, vol. 40, pp. 325–333, 2015.
- [9] Qilong Zhang and R. Pless, "Extrinsic calibration of a camera and laser range finder (improves camera calibration)," in *IEEE/RSJ International Conference on Intelligent Robots and Systems (IROS)*, vol. 3, 2004, pp. 2301–2306.
- [10] Bouguet J. Y., "Camera calibration toolbox for matlab," Tech. Rep., 2003.
- [11] R. Unnikrishnan and M. Hebert, "Fast Extrinsic Calibration of a Laser Rangefinder to a Camera," *Robotics*, 2005.
- [12] G. Li, Y. Liu, L. Dong, X. Cai, and D. Zhou, "An algorithm for extrinsic parameters calibration of a camera and a laser range finder using line features," *IEEE International Conference on Intelligent Robots and Systems*, pp. 3854–3859, 2007.
- [13] F. Vasconcelos, J. P. Barreto, and U. Nunes, "A minimal solution for the extrinsic calibration of a camera and a laser-rangefinder," *IEEE Transactions on Pattern Analysis and Machine Intelligence*, vol. 34, no. 11, pp. 2097–2107, 2012.
- [14] J. J. Craig, *Introduction to robotics: mechanics and control*, 3rd, Ed. Addison-Wesley, 1986.
- [15] M. Newville, T. Stensitzki, D. B. Allen, and A. Ingargiola, "LMFIT: Non-Linear Least-Square Minimization and Curve-Fitting for Python," 2014.
- [16] J. M. Hollerbach and C. W. Wampler, "The calibration index and taxonomy for robot kinematic calibration methods," *International Journal of Robotics Research*, vol. 15, no. 6, pp. 573–591, 1996.